Revista Latinoamericana de Metalurgia y Materiales 2008; **28** (2): 99-110

NUMERICAL SIMULATION FOR PREDICTION OF FILLING PROCESS IN A SAND MOULD

Moisés M. Pariona [1,3], Guilherme A. Salem [2], Felipe Bertelli [3], Noé Cheung [3]*

1: Pós-graduação em Engenharia e Ciência de Materiais e Departamento de Matemática e Estatística, Universidade Estadual de Ponta Grossa, UEPG Campus Uvaranas, Bloco CIPP, Laboratório LIMAC, CEP:84030900, Ponta Grossa, PR, Brazil.

2: Departamento de Física, Universidade Estadual de Ponta Grossa, UEPG Campus Uvaranas, Bloco L, Ponta Grossa, PR, Brazil.

3: Departamento de Engenharia de Materiais, Universidade Estadual de Campinas – UNICAMP Caixa Postal 6122, 13083-970, Campinas, SP, Brazil.

[*] *E-mail: mmpariona@uepg.br, moisespariona@uol.com.br*

Recibido: 16-Abr-2007; Revisado: 29-Jul-2008; Aceptado: 16-Sep-2008
Publicado On-Line: 27-Ene-2009
Disponible en: *www.polimeros.labb.usb.ve/RLMM/home.html*

Abstract

In this work, the simulation of a filling process for a mold casting was accomplished by the finite elements method. In this study, a Cu-5%Zn alloy solidified in a sand mold was used for numerical modeling. The mold filling process was simulated in atmospheric conditions under gravity and the liquid metal was poured into the mold through a mold channel. The analysis was conducted in the regions of the mold channel, in the mold and at the exit area of the mold, concerning velocity, pressure, temperature, solid fraction and the turbulent kinetic energy of the fluid. The advantage of simulations is to analyze several phenomena present in the mold filling process which are not trivial to be experimentally visualized. The simulation is a powerful tool that permits the analysis and control different parameters, in order to achieve an optimized design to attend the required quality of the cast product.

Keywords: *Casting, Mold filling, Numerical simulation, Cooper alloy, Sand mold*

Resumo

Neste trabalho foi realizada a simulação numérica do processo de enchimento de um molde pelo método de elementos finitos. Para esta finalidade foi usada uma liga Cu-5%Zn solidificada em um molde de areia. A simulação foi realizada em condições atmosféricas, sob a influência da gravidade e o enchimento do molde pelo metal líquido foi realizado através do canal de alimentação. A análise do resultado do campo de velocidade, pressão, temperatura, fração sólida e energia cinética de turbulência do fluido foi realizada nas regiões do canal de alimentação, no molde e na área externa do molde. A simulação numérica apresenta a vantagem de analisar diversos fenômenos presentes no processo de enchimento o que não é trivial pela visualização experimental. A simulação é uma poderosa ferramenta que permite analisar e controlar os diversos parâmetros deste processo com a finalidade de alcançar um projeto otimizado que atenda a qualidade desejada do produto fundido.

Palavras-Chaves*: Fundição, Vazamento, Simulação numérica, Liga de cobre, Molde de areia*

1. INTRODUCTION

Casting processes are widely used to produce metal components. The demand for high precision casting parts continues to increase due to exacting requirements from the automotive and aero-industries. Much research has been devoted toward process development for the production of high quality casting goods at low costs. From a macroscopic point of view, casting processes involve the coupling of solidification heat transfer and fluid flow. Fluid flow analysis during the mold filling process has been vigorously studied in recent decades due to the advance of computer hardware and software systems [1,2].

Numerical simulation provides a powerful means of analyzing various physical phenomena occurring during casting processes. It gives an insight into the details of fluid flow, heat transfer and solidification. Numerical solutions allow researchers to observe and quantify what is not usually visible or measurable during real casting processes. The goal of such simulations is to help shorten the design process and to optimize casting parameters to reduce scrap, use less energy and, of course, to make better castings. Simulation produces a tremendous amount of data that characterize the transient flow behavior (*i.e.* velocity, temperature), as well as the final quality of the casting (*i.e.* porosity, grain structure). It takes good understanding of the actual casting process and experience in numerical simulation for a designer to be able to relate one to the other and derive useful conclusions from the results [3].

According to the author Babaei *et al.* [4], mold filling is a very important step in determining the quality of a casting. The fluid flow phenomenon during the mold filling is closely related to the casting quality, surface finish, and macro segregation of the cast part and mold erosion. Dimensional accuracy of a casting and die life is also affected by the fluid flow in the mold cavity. In addition, the flow pattern of the metal affects the temperature distribution in the mold cavity, which is an important condition for a good solidification simulation. Modeling of the mold filling is a very complex process, since many physical phenomena, such as free surface flow, turbulence, surface tension and combination of fluid flow with heat transfer, should be considered. In order to take all these parameters into account, the computing technique tends to become complicated [4].

1.1 Governing Equations [4-7]

The mass, momentum and energy conservation equations that govern fluid flow and heat transfer can be expressed in vector calculus notation as follow:

(a) Mass conservation equation (continuity) in rectangular coordinates becomes:

$$\frac{\partial \rho}{\partial t} + \nabla . \rho \vec{v} = 0 \tag{1}$$

Where ρ is the density, $\vec{v}$=(u, v, w) the velocity, and if we assume ρ constant then

$$\frac{\partial u}{\partial x} + \frac{\partial v}{\partial y} + \frac{\partial w}{\partial z} = 0 \tag{2}$$

(b) Momentum conservation equation (Navier–Stokes), in rectangular coordinates can be expressed as [6,7]

$$\rho \left\{ \frac{\partial \vec{v}}{\partial t} + \vec{v}.\nabla \vec{v} \right\} = -\nabla P + \mu \nabla^2 \vec{v} + \rho \vec{g} \tag{3}$$

where, $\vec{P}$ is pressure, μ dynamic viscosity, $\vec{g}$ gravity, and if fluid viscosity and density were assumed constant, then Eq. 3 can be simplified.

(c) Energy conservation equation for liquid region is [6]

$$\rho c \left(\frac{\partial T}{\partial t} + \vec{v}.\nabla T \right) = k \nabla^2 T + \dot{q} \tag{4}$$

$$\dot{q} = \rho L \frac{\partial f_s}{\partial t} \quad \text{and}$$

$$f_s = \begin{cases} 0 & T > T_\ell \\ (T_\ell - T)/(T_\ell - T_s) & T_s \le T \le T_\ell \\ 1 & T < T_s \end{cases} \tag{5}$$

where c is specific heat, k thermal conductivity, $\dot{q}$ generated heat, L latent heat, f_s fraction solid, T_ℓ and T_s are, respectively, the liquidus and solidus temperature and T the temperature.

When the mold filling with fluid metal takes place, the turbulence phenomenon begins. Turbulence means that the instantaneous velocity is fluctuating at every point in the flow field. To simulate the turbulence, many mathematical models exist in the literature, as for number, there are eight turbulence models available in FLOTRAN [5,7-11]. These models acronyms and names are: Standard k-ε Model, Zero Equation Model, RNG - (Re-normalized Group Model), NKE - (New κ-ε Model), GIR, SZL, Standard k-ω Model, SST. The κ-ε model and its extensions entail solving partial differential equations for turbulent kinetic energy *κ* and its dissipation rate *ε*.

(d) The turbulent kinetic energy equation for NKE - (New κ-ε Model) is presented by following

$$\frac{\partial(\rho\kappa)}{\partial t} + \frac{\partial(\rho u \kappa)}{\partial x} + \frac{\partial(\rho v \kappa)}{\partial y} + \frac{\partial(\rho w \kappa)}{\partial z} = \frac{\partial}{\partial x}\left(\frac{\mu_t}{\sigma_k}\frac{\partial \kappa}{\partial x}\right) + \frac{\partial}{\partial y}\left(\frac{\mu_t}{\sigma_k}\frac{\partial \kappa}{\partial y}\right) + \frac{\partial}{\partial z}\left(\frac{\mu_t}{\sigma_k}\frac{\partial \kappa}{\partial z}\right) + \mu_t \Phi - \rho\varepsilon + \frac{C_4 \beta \mu_t}{\sigma_t}\left(g_x \frac{\partial T}{\partial x} + g_y \frac{\partial T}{\partial y} + g_z \frac{\partial T}{\partial z}\right) \tag{6}$$

The viscous dissipation term in tensor notation is

$$\Phi = \mu \left(\frac{\partial u_i}{\partial x_k} + \frac{\partial u_k}{\partial x_j} \right) \frac{\partial u_i}{\partial x_k} \tag{7}$$

where σ_t, is the turbulent Prandtl (Schmidt) number;

g_x, g_y and g_z, are components of acceleration due to gravity and u_i, magnitude of the velocity vector.

The turbulent viscosity is calculated as a function of the turbulent parameters kinetic energy κ and its dissipation rate ε, that is:

$$\mu_t = \rho C_\mu \frac{\kappa^2}{\varepsilon} \tag{8}$$

where, C_μ, is turbulent constant; κ, turbulent kinetic energy and ε, turbulent kinetic energy dissipation rate.

For the incompressible solution algorithm is used the equation

$$\frac{d\rho}{dP} = \frac{1}{\beta} \tag{9}$$

where, β, is the bulk modulus.

(e) The dissipation rate equation for NKE - (New k-ε Model) is presented by equation:

$$\begin{aligned}
&\frac{\partial(\rho\varepsilon)}{\partial t} + \frac{\partial(\rho u\varepsilon)}{\partial x} + \frac{\partial(\rho v\varepsilon)}{\partial y} + \frac{\partial(\rho w\varepsilon)}{\partial z} = \\
&\frac{\partial}{\partial x}\left(\frac{\mu_t}{\sigma_\varepsilon}\frac{\partial \varepsilon}{\partial x}\right) + \frac{\partial}{\partial y}\left(\frac{\mu_t}{\sigma\varepsilon}\frac{\partial \varepsilon}{\partial y}\right) + \frac{\partial}{\partial z}\left(\frac{\mu_t}{\sigma_\varepsilon}\frac{\partial \varepsilon}{\partial z}\right) + \\
&C_{1\varepsilon}\mu_t \frac{\varepsilon}{\kappa}\Phi - C_2\rho\frac{\varepsilon^2}{\kappa} + \\
&\frac{C_\mu(1-C_3)\beta\rho\kappa}{\sigma_t}\left(g_x\frac{\partial T}{\partial x} + g_y\frac{\partial T}{\partial y} + g_z\frac{\partial T}{\partial z}\right)
\end{aligned} \tag{10}$$

The new functions utilize two invariants constructed from the symmetric deformation tensor S_{ij}, and the antisymetric tensor W_{ij}. These are based on the velocity components u_k in the flow field.

$$S_{ij} = \frac{1}{2}(u_{i,j} + u_{j,i}) \tag{11}$$

$$W_{ij} = \frac{1}{2}(u_{i,j} - u_{j,i}) + C_\mu \Omega_m \varepsilon_{mij} \tag{12}$$

where, C_μ, turbulent constant; Ω_m, angular velocity of the coordinate system and ε_{mij}, alternating tensor operator. The invariants are:

$$\eta = \frac{\kappa}{\varepsilon}\sqrt{2S_{ij}S_{ij}} \quad \text{and} \quad \xi = \frac{\kappa}{\varepsilon}\sqrt{2W_{ij}W_{ij}} \tag{13,14}$$

$$C_\mu = \frac{1}{4 + 1.5\sqrt{\eta^2 + \xi^2}} \tag{15}$$

$$C_{1\varepsilon} = \max\left(C_{1M}\frac{\eta}{\eta + 5}\right) \tag{16}$$

where, $C_{1\varepsilon}$, C_2, σ_k, σ_ε, σ_t, C_3, C_4, C_{1M} and β are constants.

1.2 Free Surface Modeling

In the last years due to the technological evolution of the software and hardware, an intense study and application of the filling process of the mold by the metallic fluid was noticed in the literature.

During the mold filling process, liquid metal and air coexist in the mold and the interface position changes rapidly with time [1]. It is essential to introduce a free-surface-tracking algorithm to analyze the filling process. VOF is the most widely used method for free-surface tracking in mold filling [1]. In a three dimensional rectangular coordinate frame, the transport equation on the VOF, F(**r**,t), for an incompressible fluid can be written as:

$$\frac{\partial F}{\partial t} + \nabla F.\vec{v} = 0 \tag{17}$$

The F(**r**,t) function governed by the above equation is unity in the fluid occupied region and zero in the empty region. For the given computational domain, the F(**r**,t) field obtained from Eq. 17 gives the information for the free surface. The cells with F(**r**,t) values between 0 and 1 are the free surface cells. The VOF method has been applied successfully to many engineering problems involving free surfaces including a mold filling problem. However, since the original VOF method uses an explicit differencing method in time, large computational time is required to analyze a typical filling problem.

The author Im *et al*. [1] affirmed, that is more efficient to use a time-implicit VOF method to alleviate the severe time step restriction than the time-explicit VOF method. The time implicit VOF method [1] is based on the assumption that a cell being filled cannot transmit fluid to its neighboring cells until it is completely filled. Once the cell is filled, it can transmit fluid to neighboring cells.

The numerical method used to analyze fluid flow and thermal behavior during and after filling in the mold is described as follows [1]. Continuity, momentum, energy and F(**r**,t)-transport equations are discretized using the fully implicit method in time. First, the velocity and pressure fields are obtained from the momentum and continuity equations. Then the new fluid configuration is computed from Eq. 17. The energy equation is solved for the fluid-occupied region to determine the temperature and the liquid fraction. The updated values of F(**r**,t) are utilized to modify the velocity and pressure, and then the temperatures and liquid fractions are updated based on the modified velocity and pressure. This iteration procedure is repeated until the total fluid volume and temperature changes are small enough to satisfy the prescribed convergence criteria. If the convergence criterion is satisfied, the time is advanced. This time-implicit VOF method is adopted to reduce the tremendous computation time that is required when the original VOF method is used [1].

According to Kermanpur *et al*. [3], mould filling problems involve tracking free surfaces that are the boundaries between liquid metal and the surrounding air. The most common used method to describe free surfaces is the volume-of-fluid (VOF) method. The VOF method enables tracking the transient-free surfaces with arbitrary topology and deformations (*i.e.*, fluid surface break-up and coalescence). The 'true' VOF method consists of three main components:

1. A fluid fraction function F(**r,t**) which is equal to 1.0 in fluid regions, and equal to 0.0 in voids. Since fluid configurations may change with time, F(**r**,t) is a function of time, *t*, as well as space, **r**. Averaged over a computational control volume, the fluid fraction function has a fractional value in cells containing a free surface.
2. Zero shear stress and constant pressure boundary conditions are applied at free surfaces.
3. A special advection algorithm is used for tracking sharp free surfaces.

The boundary conditions at the free surface are zero normal and tangential stresses.

A free surface advection method must preserve the sharpness of the interface and have minimal free surface distortion. Generally, such advection algorithms are based on geometric reconstruction of the free surface using the values of F(**r**,t) at grid nodes [3]. Sometimes a free surface is approximated by a density discontinuity between metal and air, then, flow equations are solved for both fluids. In that case it is difficult to enforce correct boundary conditions at the surface. This is because free surface pressure and velocities in the two-fluid approach are not set explicitly, but are computed by solving the flow equations and these flow equations are solved in terms of mixture variables. Since densities of liquid metal and air differ greatly (*i.e.*, by a factor of 7000 for steel), the mixture velocity may not always be an accurate measure of the relative motion of metal and air [3].

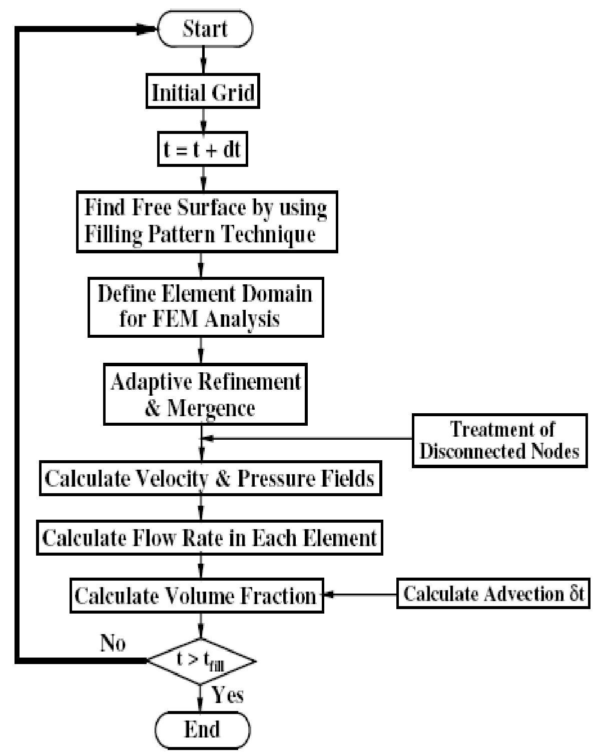

Figure 1. Flow chart of computational procedure [12].

The authors Kim *et al*. [12] presented a flow chart of computational procedure of the mold filling process. Figure 1 shows the computational procedure for the filling stage of the casting process. In the first stage of numerical analysis, an initial grid is generated and values for the order of surface refinement, material properties, boundary conditions, and initial volume fractions are the input. Then the time step is increased and the filling pattern is selected for each element, and the free surface is predicted by the filling pattern. In the next stage, through the refinement and mergence procedure, an adaptive grid is generated. According to the volume fraction at the given moment of change in filling, the element domain for the FEM analysis is created. Then, by the FEM analysis, the velocity and pressure fields are obtained and the flow rate in each element is calculated. Subsequently the procedure of advection treatment is accomplished and the volume fraction in each element is obtained. These procedures are iterated until the current filling time reaches the total time.

To perform the filling pattern technique, free surfaces are tracked through volume tracking methods by involving fluid volumes forward in time with solutions of the advection equation. At any time in the solution of the Eulerian method, the information of the exact surface location is not known [12]. An obtained distribution of volume fraction data does not guarantee a unique free surface. Instead, the free surface must be inferred, based on local volume data and the assumptions of a particular algorithm, before the free surface scan be reconstructed. Then the reconstructed free surface is used to calculate the flow rate in the element to integrate the volume transient equations [12].

One of the requirements that should be satisfied, is the conservation of the F(r,t) function even though with the presence of convection. This method uses minimum of stored information and it follows regions rather than boundaries, which avoids the logic problems associated with intersecting surfaces. The derivatives of this function can be used to estimate the orientation of the fluid surface and finally improvement in computation efficiency [4]

In this study, the numeric simulation of the mold filling with the Cu-5%Zn alloy was accomplished in a sand mold. For this purpose, the finite elements method and the software ANSYS were applied. The properties such as density, specific heat and viscosity of the alloy were considered constant, but the thermal conductivity of this alloy varies according to the temperature. The properties of the mold material were considered constant. For the simulation, the turbulence, gravity and incompressible fluid were considered, and the time of mold filling was of 3 s. As result, the velocity of the flow, the variation of the pressure, heat transfer, as much in the mold as in the furnace were determined, and also the volume fraction and turbulence kinetic energy were determined.

2. METHODOLOGY OF THE NUMERICAL SIMULATION

The filling process of the mold by the liquid metal is followed according to the authors' explanations Im *et al.* [1] and Kim *et al.* [12]. First, some initial conditions were established such as temperature, pressure and VOF in the elements of the mesh, as mentioned in the methodology of the numeric simulation. Through FEM, the velocity and pressure fields were obtained from the continuity (Eq. 2) and momentum (Eq. 3) equations. Then the new fluid configuration is computed according the transport equation on the VOF, F(**r**,t) (Eq. 17). The energy equation (Eq. 4) is solved for the region occupied by the fluid in order to determine the temperature. Subsequently, the procedure of advection treatment is accomplished and the volume fraction in each element is obtained. After, the turbulent kinetic energy equation is solved for NKE from Eq. 10. The updated values of F(**r**,t) are used to modify the velocity and pressure, and then the temperatures and liquid fractions are updated based on the modified velocity and pressure.

The considered geometric model is represented in Figure 2. The dimensions of the model are in m. In this figure we can observe that between the exit of the furnace and the entrance of the mold there is a free space of 0.1 m. Not only this free space but also the exit of the furnace is exposed to the environment. To reach the convergence according to the condition of the (VOF) algorithm, the geometry of the mesh element is quadrilateral form and the mesh of the mold channel must have continuity, as it can be observed in Figure 2.

The properties of the materials, such as of the liquid metal and of the sand mold are presented in Table 1. In order to simulate the liquid metal flow inside the sand mold, the following conditions were considered: (a) the liquid metal and the sand mold were stabilized in normal condition of atmospheric pressure; (b) the initial temperature of the liquid metal was 1550 K and the temperature of the mold was the same temperature of the environment (c) the velocity of the liquid was fastened in zero on the walls of the mold; (d) the mathematical model for the turbulence NKE Model [5] was considered. The constants for this model were presented in Table 2, (e) VOF algorithm was used for mold filling. An artifice in the VOF technique was applied to describe the mold wall as a region not allowed to be filled by the liquid: The VOF for the mold wall was considered 1 (light gray color). According to Figure 2, the dark gray color regions represent the places that could be filled by the liquid and their VOF values are 0. In this sense, during the dynamic of the filling, the color of the mold cavity gradually becomes light gray color (VOF=1), *i.e.*, the same color of the mold wall, (f) the total time for mold filling of the liquid metal into the mold was of 3 s

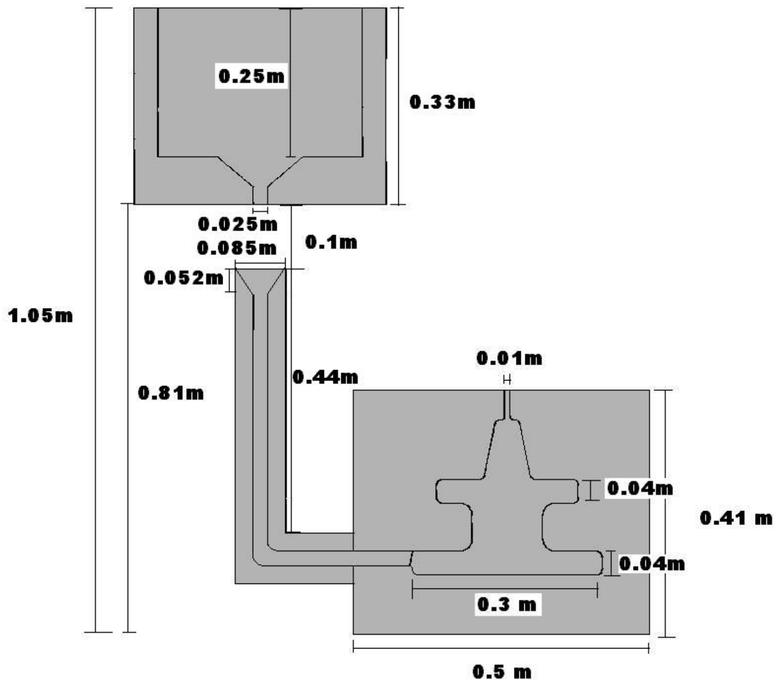

(*a*)

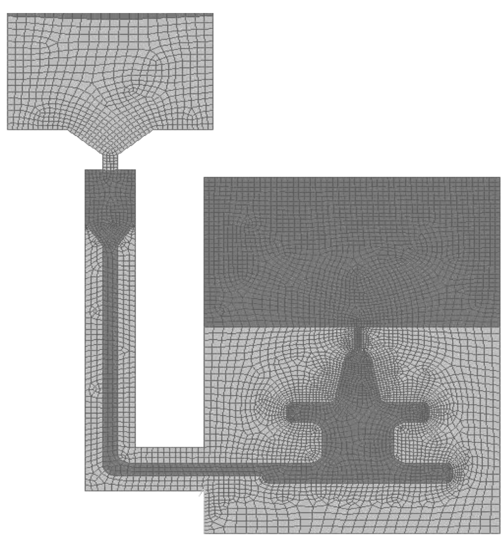

(*b*)

Figure 2. (*a*) Geometry of the model and (*b*) 2D mesh of the model.

and step time was of 0.05 s (g) the number of iterations by step was 30, (j) the properties of the materials were informed and the mesh of the model was made, and (k) the solution in 2-D was considered.

Table 1. Properties of the materials

Properties	*Value*
Industrial sand [13]	
Density (kg/m^3)	1500.00
Specific heat (J/kg.K)	900.00
Thermal conductivity (W/m.K)	0.05
Cu-5%Zn [14]	
Density (kg/m^3)	7841.18
Specific heat (J/kg.K)	492.86
Viscosity (Pa.s)	0.0034
Thermal conductivity (W/m.K) (to different temperatures (K))	314.29 (1321.46)
	307.14 (1323.77)
	300.00 (1326.08)
	292.86 (1328.38)
	278.57 (1330.69)
	257.14 (1333.00)
	228.57 (1335.31)
	178.57 (1337.62)
	107.14 (1342.23)
	107.14 (1376.85)
	107.14 (1399.92)
	107.14 (1423.00)

Table 2. NKE turbulence model coefficients adopted in this article [5]

Coefficients	*Values*
$C_{1\varepsilon}$	1.44
C_2	1.92
σ_k	1.0
σ_ε	1.2
σ_t	0.85
C_3	1.0
C_4	0.0
C_{1M}	0.43
β	0.0

To accomplish the solution process of Equations 1, 2, 3, 4, 5, 6, 10 and 17 the finite elements method and the software ANSYS [5] were used. Specific heat and viscosity were considered constant and incompressible fluid condition was considered. The most appropriate technique to generate the pressure field was Preconditioned Conjugate Residual Method and for the velocity was Tri-diagonal Matrix Algorithm [5]. The convergence in each iteration was controlled through the norm of the solution parameters [5,15,16].

3. RESULTS AND DISCUSSION

As result of this research, the different parameters that correspond to the mold filling process were determined. These parameters were calculated for the mold filling times of 1, 2 and 3 seconds. In Figure 3 the result of the fluid velocity (m/s) is shown in magnitude, as well as in vectorial form. It is observed that the velocity varies in function of the trajectory, being higher on the first second. It is also observed that the fluid leaves out the mold. For 1s and 2s, high turbulence is noticed in the curvatures of the mold geometry. When the liquid is liberated from the mold at the time of 2 s, an abrupt exit of the fluid occurs and for 3 s the mold is completely filled and some melt flows through the mold exit. This phenomenon happens due to the abrupt variation of the pressure, because it changes from high to the atmospheric pressure. In sequence, the liquid starts to slide on the external surface of the mold. This phenomenon was better reproduced in this work by the turbulence model NKE [5. Other turbulence models were applied, but they did not succeed in reproducing the phenomenon adequately.

In Figure 4 the pressure variation is showed in the mold channel and in the mold. In the first second in the sprue base a maximum pressure of 139732 Pa is presented. In the time of 2 s a maximum pressure of 138005 Pa in the right inferior part of the mold is presented. In the time of 3 s, in the same point of the mold as considered for 2 s, the pressure lowers to 134280 Pa. The largest variation of the pressure is observed for the time of 2 s and as the liquid metal is cooling on the time of 3 s, the pressure in the mold decreases.

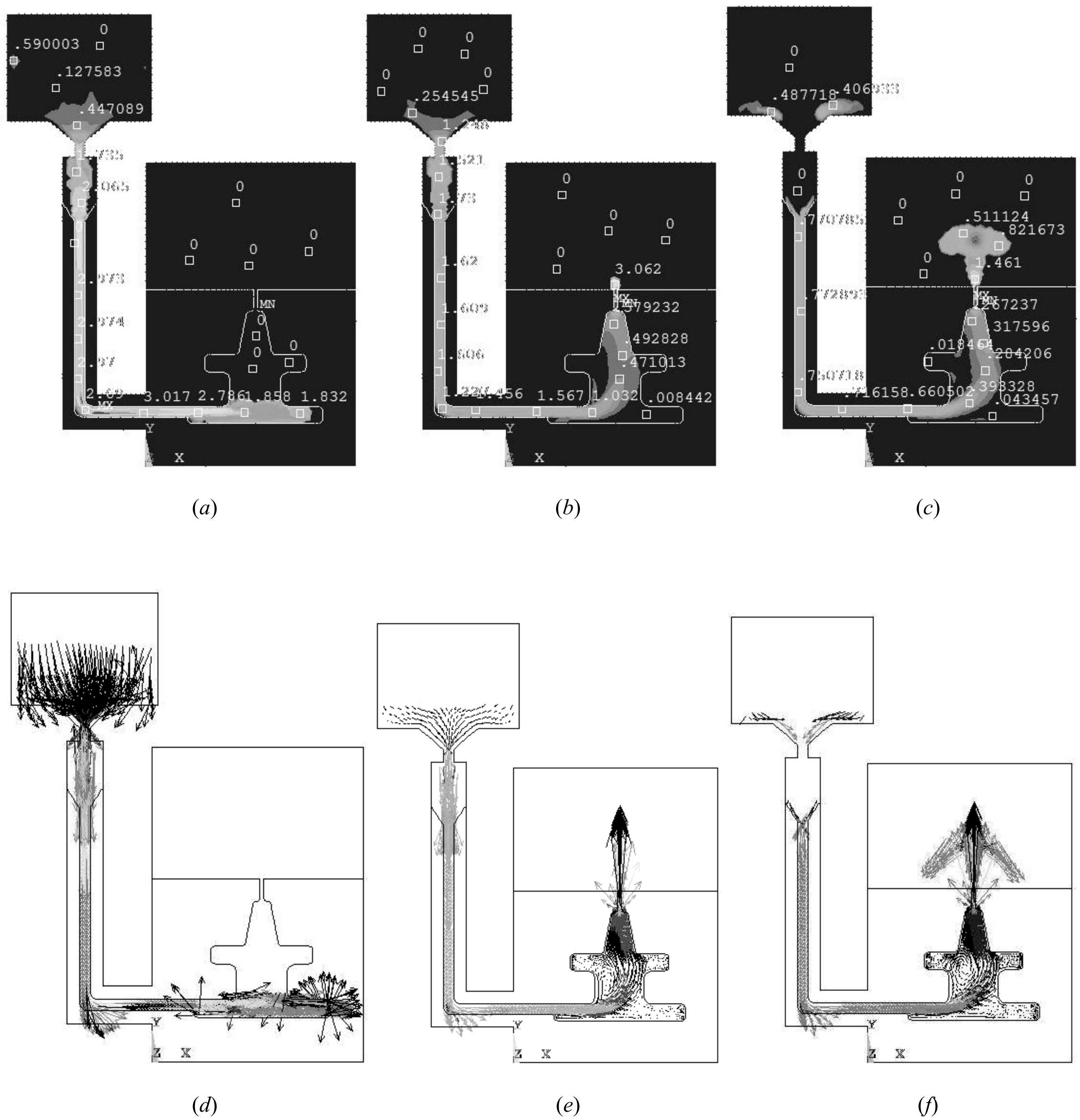

Figure 3. Velocity variation in magnitude form: (*a*) 1 s, (*b*) 2 s, (*c*) 3 s, and vectorial form: (*d*) 1 s , (*e*) 2 s, (*f*) 3 s during the mold filling.

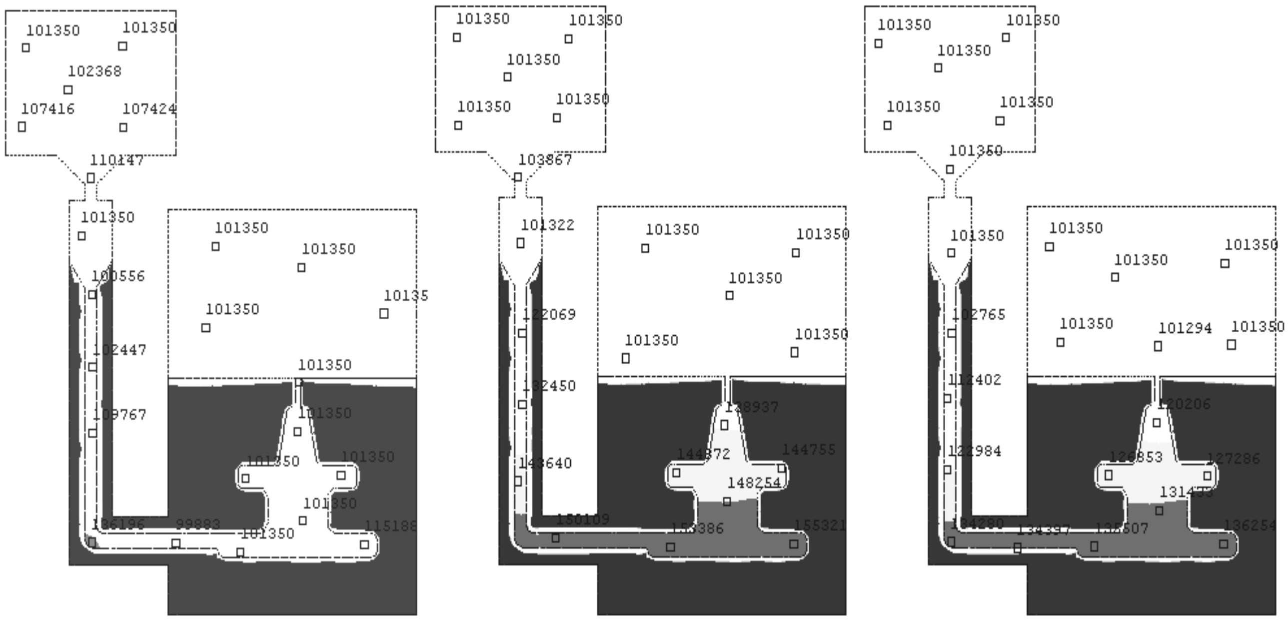

(*a*) (*b*) (*c*)

Figure 4. Pressure variation during the mold filling in (*a*) 1 s, (*b*) 2 s and (*c*) 3 s.

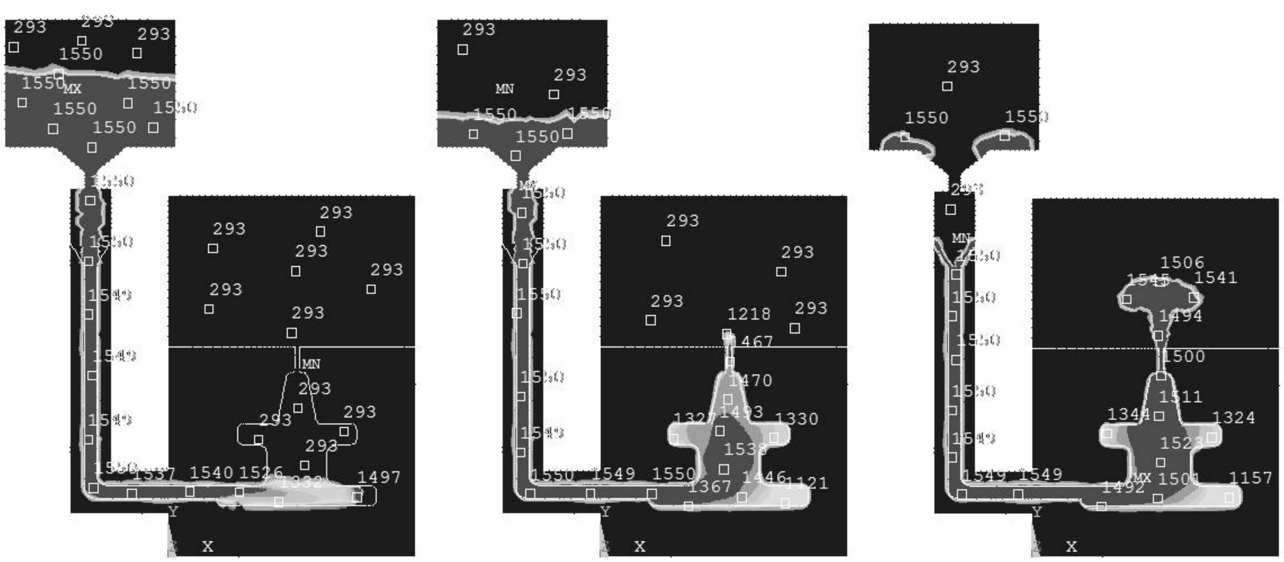

(*a*) (*b*) (*c*)

Figure 5. Temperature variation during the mold filling in (*a*) 1 s, (*b*) 2 s and (*c*) 3 s.

Another result calculated in this study was the variation of the temperature during the mold filling, as shown in Figure 5. It is observed that the temperature decreases around 300 K in the first curvature in the right inferior part of the mold for 1 s. In a general way, in all the curvatures where the fluid exists, an appreciable cooling is presented, for instance, a cooling around 350 K for 2 s in the right inferior part of the mold. For the instance of 2 s, the simulation showed that the liquid jet encountered a path free from furnace to the mold exit and as shown in Figure 3*c* and 3*f*, the liquid did not fill the lateral cavities of the mold, avoiding turbulence. In this sense, the heat losses caused by convection effect can be neglected and due to this fact, the expelled fluid from the mold presents a high temperature (Figure 5*c*), close to the pouring temperature (1550 K).

The volume fraction was calculated, as it is shown in Figure 6, where the gray color represents the cell filled by liquid with a value of unity and the dark gray the empty cell with a value of zero. For 1 s, some empty areas exist, for 2 s a uniform filling was observed in the whole volume of the mold and a drop came out from the mold.

The macrostructure defects, as shrinkage, macro segregation, mold erosion, etc. [1,3,15] depend on the way of filling of the mold, the quality of the fluid flow in the mold cavity, the height of the furnace in relation to the mold, the turbulence, the superheating temperature of liquid metal, the filling velocity, the surface tension, the initial condition of pressure and temperature inside of the mold and on the turbulence model. The volume fraction is an important parameter that characterizes the mold filling quality and that predict the macrostructure defects.

Finally, the turbulent kinetic energy (Joule) was obtained. It is shown in Figure 7, where a great variation of this parameter is observed for the times of 1 and 3 s of mold filling. The great variation of turbulent kinetic energy is related to the great variation of the fluid velocity and this is also related to the larges variation of turbulence (Figure 3).

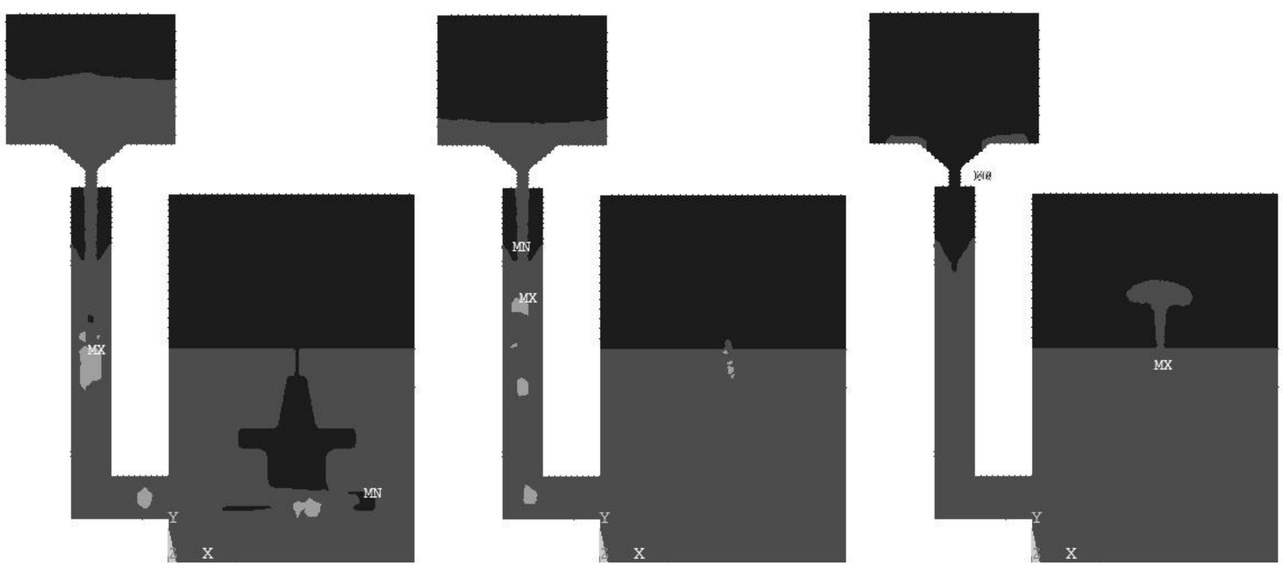

(*a*) (*b*) (*c*)

Figure 6. Volume fraction during mold filling in (*a*) 1 s, (*b*) 2 s and (*c*) 3 s.

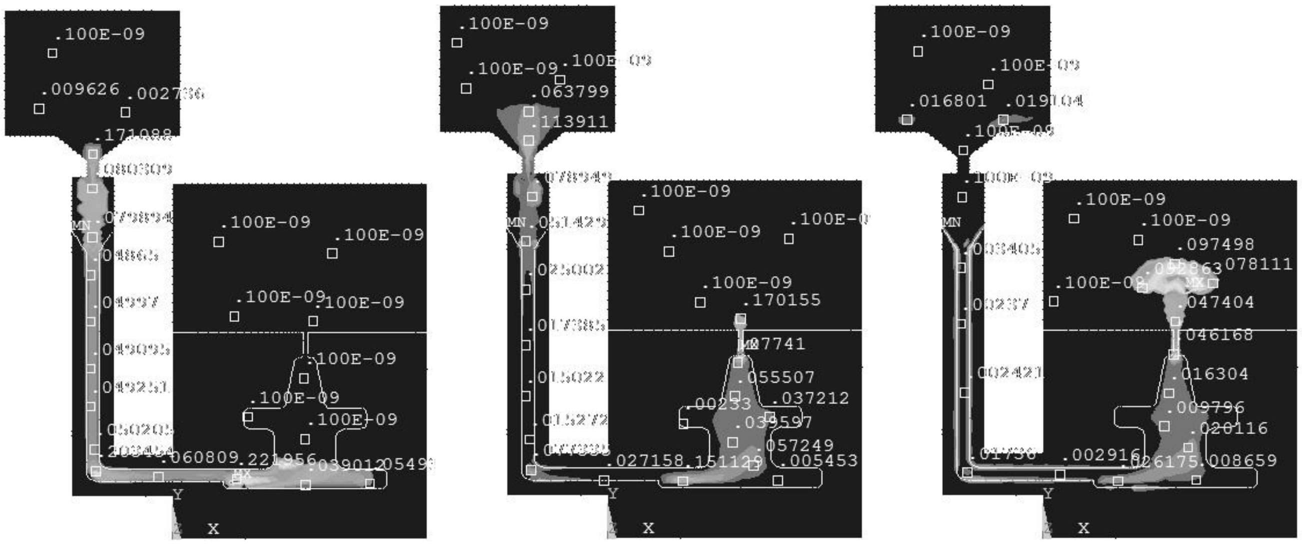

(*a*) (*b*) (*c*)

Figure 7. Turbulent kinetic energy during mold filling in (*a*) 1 s, (*b*) 2 s and (*c*) 3 s.

The free surface of the overflow at the dead-end-like corner entering the mold cavity (sprue base) was avoided through an analysis of proper geometry of the system and its dimensions, *i.e.*, mold channel height; inclination of the pouring basin; diameter of the furnace exit; height between furnace exit and the pouring basin; proper curvature of the sprue base. In addition, due to the complex geometry of the cast system, it is necessary to use adequate finite element geometry. In this study, a quadrilateral element denominated “141” was used, which is indicated to deal with the filling mold process.

4. CONCLUSIONS

The filling process of the mold by liquid was analyzed for three instants of time. In this process different phenomena were presented, such as variation of the velocity in the mold channel and in the mold and presence of turbulence, especially in the curved parts of the mold. On the exit of the mold in 2 s, an abrupt detachment of the liquid metal was presented. Also, pressure variation was observed in the whole system, especially for the mold filling time of 2 s. The variation of the temperature was appreciable in the greater curvatures of the mold, due to the stagnated liquid in these areas. For the time of 3 s, the liquid metal is reheated in these areas, due to the flow of the fluid that feeds the mold.

The finite elements method is a powerful mathematical tool to analyze mold filling process that is not trivial to visualize experimentally. The simulation permits to visualize the filling dynamics and to control the process, varying the operational parameters. For the sake of competitiveness on the world market, the practice of simulation and mathematical modeling in casting industry can produce a series of benefits such as optimization, time saving, waste minimization, and cast final quality improvement.

5. ACKNOWLEDGEMENTS

The authors acknowledge financial support provided by CNPq (The Brazilian Research Council) and Capes - Coordenação de Aperfeiçoamento de Pessoal de Nível Superior.

6. REFERENCES

[1] Im I-T, Kim W-S, Lee K-S, *Int. J. Heat Mass Tran.* 2001; **44** (8): 1507-1515.

[2] Mirbagheri SMH, Esmaeileian H, Serajzadeh S, Varahram N, Davami P, *J. Mater. Process. Tech.* 2003; **142** (2): 493–507.

[3] Kermanpur A, Mahmoudi Sh, Hajipour A, *J. Mater. Process. Tech.* 2008; **206** (1-3): 62-68.

[4] Babaei R, Abdollahi J, Homayonifar P, Varahram N, Davami P, *Comput. Methods*

Appl. Mech. Engrg. 2006; **195** (7-8): 775-795.

[5] *Handbook Ansys*. Canonsburg (EE.UU.): Ansys Inc., 2007.

[6] Son G, Dhi VK, *Int. J. Heat Mass Tran.* 2008; **51** (5-6): 1156–1167

[7] Zaidi K, Abbes B, Teodosiu C, *Comput. Methods Appl. Mech. Engrg.* 1997; **144** (2-3): 227-233.

[8] Felicelli SD, Heinrich JC, Poirier DR, *J. Cryst. Growth* 1998; **191** (4): 879-888.

[9] Reza Aboutalebi M, Guthrie RIL, Seyedein SH, *Appl. Math. Model.* 2007; **31** (8): 1671-1689.

[10] Sharma AK, Velusamy K, Balaji C, *Ann. Nucl. Energy* 2008; **35** (8): 1515-1518.

[11] Cheng TS, Yang WJ, *Comput. Fluids* 2008; **37** (3): 194–206.

[12] Kim KD, Yang DY, Jeong JH, *Comput. Methods Appl. Mech. Engrg.* 2006; **195** (48-49): 6799-6821.

[13] Kingery WD, Bowen HK, Uhlmann DR, *Introduction to Ceramics*, 2nd Ed. New York (EE.UU.): John Wiley & Sons Inc, 1976.

[14] Miettinen J, *Comp. Mater. Sci*. 2001; **22** (3): 240-260.

[15] Pariona MM, Mossi AC, *J. Braz. Soc. Mech. Sci. & Eng*. 2005; **27** (4): 399-406.

[16] Mossi AC, Pariona MM, *Rev. Téc. Ing. Univ. Zulia* 2006; **29** (3): 197-208.